CrossMark

2-methylfuran Oxidation in the Absence and Presence of NO

Katiuska Alexandrino[1] · Ángela Millera[1] ·
Rafael Bilbao[1] · María U. Alzueta[1] (iD)

Abstract 2-methylfuran (2-MF) has become of interest as biofuel because of its properties and the improvement in its production method, and also because it is an important intermediate in the conversion of 2,5-dimethylfuran. In this research, an experimental and kinetic modelling study of the oxidation of 2-MF in the absence and presence of NO has been performed in an atmospheric pressure laboratory installation. The experiments were performed in a flow reactor and covered the temperature range from 800 to 1400 K, for mixtures from very fuel-rich to very fuel-lean, highly diluted in nitrogen. The inlet 2-MF concentration was 100 ppm. In the experiments in the presence of NO, the inlet NO concentration was 900 ppm. An interpretation of the experimental results was performed through a gas-phase chemical kinetic model. A reasonable agreement between the experimental trends and the modelling data is obtained. The results of the concentration profile of 2-MF as a function of temperature indicate that, both in the absence and in the presence of NO, the onset of 2-MF consumption is shifted to lower temperatures only under fuel-lean and very fuel-lean conditions. Furthermore, under these conditions the presence of NO also shifts the onset of 2-MF consumption to lower temperatures. The effect of the 2-MF presence on the NO reduction varies with the oxygen concentration. It is seen that under very fuel-rich and stoichiometric conditions NO is reduced basically by reburn reactions, while under fuel-lean and very fuel-lean conditions, the NO-NO$_2$ interconversion appears to be dominant.

✉ María U. Alzueta
uxue@unizar.es

[1] Aragón Institute of Engineering Research (I3A), Department of Chemical and Environmental Engineering, University of Zaragoza, Río Ebro Campus. 50018 Zaragoza, Spain

⌖ Springer

1 Introduction

Furan derivatives have recently gained a special interest as it is believed they may be a good alternative as new biofuels. 2,5-dimethylfuran (2,5-DMF, C_6H_8O) and 2-methylfuran (2-MF, C_5H_6O) have an special importance due to the improvement in their production method through the conversion of fructose, glucose, and even cellulose [1–3]. Moreover, 2-MF is a product formed in both the pyrolysis and oxidation of 2,5-DMF. This work is focused on 2-MF. Research on 2,5-DMF oxidation, and its interaction with NO can be found in our previous publications [4, 5].

2-MF has attractive properties as biofuel, it has even several advantages over ethanol, the currently more used biofuel. For example, its higher rate of vaporization and higher combustion stability make it more robust to cold engine start than ethanol [6]. In this way, the potential of 2-MF as biofuel has been already investigated in spark ignition (SI) engines [6, 7]. Wang et al. [8] studied the combustion characteristics and emissions of 2-MF compared to 2,5-DMF, gasoline and ethanol in a direct injection spark ignition (DISI) engine. They found that the overall regulated emissions (CO, HC (unburned hydrocarbons), NO_x and PM (particulate matter)) from 2-MF are comparable to the other tested fuels, whereas the aldehyde emission is much lower than the obtained from gasoline and ethanol. To our knowledge, 2-MF has not yet been studied in diesel vehicles.

As a biofuel candidate, a better understanding of the combustion of 2-MF is necessary. Grela et al. [9] studied the decomposition of furan, 2-MF and 2,5-DMF in a heated flow reactor operating at very low pressures (1 mtorr) and temperatures of 1050-1270 K. Lifshitz et al. [10] studied the decomposition of 2-MF behind shock waves in a pressurized driver single pulse shock tube over the temperature range 1100-1400 K. More recently, the combustion intermediates in 2-MF premixed flames [11], laminar burning characteristics [12, 13], ignition delays in shock-tube [14–17] and computational study of the combustion and atmospheric decomposition of 2-MF [18], have been studied. Somers et al. [19] conducted an experimental and modelling ignition delay time study for 2-MF for different equivalence ratios (0.5, 1, and 2) in the 1200-1800 K temperature range, and laminar burning velocities were also determined for mixtures of 2-MF at equivalence ratios of 0.55-1.65 in the 298-398 K temperature range. The authors used these experimental results to validate a chemical kinetic mechanism which describes the 2-MF oxidation. In this mechanism, Quantum-Rice-Ramsperger-Kassel (QRRK) theory with a Modified Strong Collision (MSC) approach was utilized to account for the influence of pressure on reaction rate constants. The reactions of hydrogen atoms with the fuel were highlighted as important. Specifically, through sensitivity analysis, they found that the H-abstraction by hydrogen atoms promotes reactivity while the H-addition at the C2 site of 2-MF inhibits it. This model has been used in recent studies addressing the ignition phenomena of 2-MF [14, 15]. Continuing with this work, Somers et al. [20] described, in a more complete way, the *ab initio* calculations in which their original model [19] was based. Here the authors used more rigorous Rice-Ramsperger-Kassel-Marcus (RRKM) theory calculations coupled with an energy grained Master Equation (ME) solution to account for the influence of pressure on reaction rate constants. The new kinetic mechanism developed was validated with different experimental results from literature (e.g. [10, 14])

A series of three papers jointly consider the combustion chemistry of furan [21] and its alkylated derivatives: 2-MF [22] and 2,5-DMF [23], under premixed low-pressure flame conditions using molecular-beam mass spectrometry and gas chromatography. The reaction mechanism used in this series of papers [21–23] is based on a previous mechanism

by Sirjean et al. [24] which was developed to describe the combustion of 2,5-DMF. This mechanism [24] includes the furan oxidation sub-mechanism of Tian et al. [25] and a 2-MF oxidation sub-mechanism based on analogies with 2,5-DMF and furan reactions. In the above mentioned series of fuel studies [21–23], some of the reactions or rate parameters of the furan and 2-MF sub-mechanisms in the Sirjean et al. [24] model were updated or replaced to improve the simulation of some intermediates, while the 2,5-DMF sub-mechanism was not changed. Through this modified mechanism [21–23], the authors found that the H-addition pathways played an important role in the 2-MF consumption and species formation. Continuing with the work of Tran et al. [22], Moshammer et al. [26] studied the premixed combustion of 2-MF by measuring oxygenated and hydrocarbon intermediates, using synchrotron-generated vacuum-ultraviolet photons in combination with a high-resolution mass spectrometer. The experimental data are compared with modelling calculations using the combustion chemistry model employed in the series of three papers [21–23] with success. However, many experimentally newly detected species such as fulvene, C_5H_4 isomers (pentatetraene, ethynylallene, 1,3-pentadiyne, and 1,4-pentadiyne), C_3H_8O isomers (1- and 2-propanol and ethyl methyl ether), vinyl ketene ($CH_2CHCHCO$), etc., are not included in the model from Tran et al. [22], thus the results of these species could not be compared with modelling results.

It is important to study the oxidation of 2-MF, but also to study the effect of the presence of typical contaminants existing in the combustion chamber of engines, as for example NO, on the oxidation of 2-MF, as well as to study if the presence of 2-MF is able to reduce the concentration of these contaminants, in this case NO. Thus, in this work we have investigated the 2-MF oxidation in the absence and in the presence of NO. The inlet 2-MF and NO concentrations were 100 and 900 ppm, respectively, which correspond to an inlet C/N ratio of 0.56. All the experiments were carried out in a quartz flow reactor at atmospheric pressure, in the temperature range 800-1400 K, for different air excess ratio values ($\lambda = 0.3$, 1, 5 and 50), which is defined as the inlet oxygen concentration divided by the oxygen necessary for complete combustion. Thus, the influence of the oxygen concentration on the oxidation of 2-MF and on the NO consumption can be evaluated. The main reactions involved in the oxidation of 2-MF in the presence and absence of NO, as well as, in the NO consumption, have been identified by interpreting the experimental results in terms of a detailed chemical kinetic model. With this paper, in addition to show the influence of the presence of NO on the 2-MF oxidation and show if 2-MF is capable to reduce the NO concentration under different oxidizing conditions, we provide experimental data that can be used to further refine chemical kinetic models for 2-MF.

2 Experimental Approach

Experiments were performed in an atmospheric pressure facility previously used and described [e.g. 27, 28]. Briefly, the quartz flow reactor employed, with an inner diameter of 8.7 mm and a reaction zone of 200 mm in length, was designed for obtaining plug flow conditions [29]. This reactor is placed in a three-zone electrically heated furnace. The flat temperature profile is within ±10 K. The gases are led to the reactor through calibrated mass flow-controllers in four separate streams: a main flow, which contains water vapor and nitrogen, and three injector tubes, through which 2-MF, O_2 and NO (this last when applicable) are supplied. Water vapor is injected saturating a N_2 stream through a water bubbler. N_2 is used to close the balance, i.e, to achieve a total flow rate of 1000 mL(STP)/min. To achieve

a well-defined reactor volume, the main flow and the three injector flows are heated separately and mixed in cross-flow at the reactor inlet. The residence time, for the given total flow rate and a constant volume of the reaction zone is, $t_r(s)=195/T(K)$.

The gas outlet stream is cooled using cold air, and passes through a condenser and filter for conditioning. The concentration of 2-MF, NO and some products, including some nitrogen species, was analyzed by using an Agilent 3000A microchromatograph (2-MF, H_2, CO, CO_2, C_2H_4, C_2H_2), an ABB continuous Uras 14 IR for CO/CO_2 and Uras 26 IR for NO, and Mattson Fourier Transform Infrared (FTIR) spectrometer (NO, NO_2, N_2O, HCN and NH_3). The uncertainty of the concentration measurements is estimated as ±5 %, except for the FTIR spectrometer, which is estimated as ±10 %.

The experimental specifications are gathered in Table 1. The oxygen concentration is varied for air excess ratio values ranging from 0.3 to 50. 900 ppm of NO is used in the experiments of 2-MF oxidation in the presence of NO, corresponding to an inlet C/N ratio value of 0.56, which is similar to previous studies in our group [e.g. 28], and this NO concentration can be representative of real combustion processes [30, 31]. All the experiments are performed under very diluted conditions to prevent heat release, so an isothermal reaction zone is guaranteed.

3 Kinetic Modelling

The mechanism used as starting point is that compiled and used in our previous studies on the 2,5-DMF oxidation in the presence and absence of NO [4, 5]. That mechanism has been progressively develop in our group, and includes the conversion of C_1/C_2 hydrocarbons and their interaction with NO, the conversion of different oxygenated hydrocarbons, as well as other compounds of interest [27, 28, 32–36]. To this mechanism, the sub-mechanisms for furan, 2,5-DMF, 2-MF, and other intermediates from the work of Sirjean et al. [24] were added and used in the previous works [4, 5].

As a first stage, and in order to evaluate different reactions sub-mechanisms available in the literature for 2-MF conversion, in the present work three different 2-MF sub-mechanisms were incorporated separately in our base mechanism, resulting in: 1)

Table 1 Experimental conditions: [C_5H_6O]=100 ppm, T=800-1400 K, Flow rate=1000 mL(STP)/min, and $t_r(s)=195/T(K)$. N_2 is used to close the balance

Set	O_2 (ppm)	λ	NO (ppm)	H_2O (ppm)	C/N Molar ratio
1	180	0.3	0	6343	
2	180	0.3	900	6343	0.56
3	600	1	0	8108	
4	600	1	900	8108	0.56
5	3000	5	0	6343	
6	3000	5	900	6343	0.56
7	30000	50	0	6748	
8	30000	50	900	7629	0.56

mechanism 1, incorporates in the base mechanism developed by our group the 2-MF sub-mechanism by Sirjean et al. [24]; 2) mechanism 2, includes the 2-MF sub-mechanism by Tran et al. [22], which is the same sub-mechanism used in the mechanism 1, in which the authors, changed some kinetic parameters for certain reactions in order to improve low-pressure premixed flames results. The authors also add to this sub-mechanism an H-atom addition reaction on the C2 site of 2-MF, yielding 1,3-butadiene ($CH_2CHCHCH_2$) and the HCO radicals. Finally, 3) mechanism 3 incorporates to the base mechanism developed in our group, the 2-MF sub-mechanism from Somers et al. [20], in which an *ab initio* study was carried out to calculate kinetic parameters for the 2-MF sub-mechanism, and accounts for the influence of pressure on reaction rate constants. The SENKIN computer code from the CHEMKIN package [37] was used to simulate the experimental data. The sensitivity analysis was performed using the CHEMKIN-PRO package [38].

Mechanisms 1, 2, and 3 have been used to simulate the present experimental results, and the comparison of some selected results is shown here in Figs. 1, 2, 3, whereas other results can be seen in Figs. S1-S7 in Online Resource.

In Figs. 1, 2, 3, concentration profiles of 2-MF, CO and CO_2, as a function of temperature, obtained in the 2-MF oxidation in the absence of NO for $\lambda = 0.3, 5$, and 50, are compared with modelling calculations. Figure 1 reveals that the three mechanisms capture the 2-MF consumption under very fuel-rich conditions ($\lambda = 0.3$) with good accuracy. Also the three mechanisms follow the same trend for the CO and CO_2 formation. However, none of them fits well the experimental data. This last observation is also applied to the concentration profiles of H_2, C_2H_4 and C_2H_2, which can be observed in Fig. S1 in Online Resource. With regard to stoichiometric conditions ($\lambda = 1$) in the absence of NO, which comparison between experimental results and modelling calculations can be observed in Fig. S2, the three models fit well the 2-MF, CO, and CO_2 experimental results. However, the three mechanisms overestimate the H_2 concentration values. The observations found for $\lambda = 0.3$ and 1 in the absence of NO can be extended to the case of the 2-MF oxidation in the presence of NO (Figs. S3 and S4).

Figure 2 shows that, for the 2-MF oxidation under fuel-lean conditions ($\lambda = 5$) in the absence of NO, the calculations of mechanisms 2 and 3 are closer to the experimental results than the calculations of mechanism 1, with a slightly better fit by the mechanism 3. Nevertheless, in the presence of NO, there is a poor fit to the experimental data by any of the three mechanisms (Fig. S5).

Comparing the experimental results obtained in the 2-MF oxidation under very fuel-lean conditions ($\lambda = 50$) in the absence of NO with the modelling calculations, Fig. 3 indicates that, in general, the mechanisms 1 and 2 present very close results and fit better with the experimental data than the mechanism 3, although this last mechanism fits better the experimental results when the NO is present (Fig. S6).

In Fig. S7, the performance of the different mechanisms adjusting to the experimental results of the NO concentration can also be observed. In general, the three mechanisms have the same performance, but for very fuel-lean conditions the mechanism 3 fits better the experimental results.

Taking into account the results obtained, we have chosen mechanism 3 to analyze the experimental results in the rest of the manuscript. As mentioned previously, the 2-MF conversion sub-mechanism by Somers et al. [20] has been validated with different experimental data from literature covering shock tube [10, 14] and premixed flames [22] experiments.
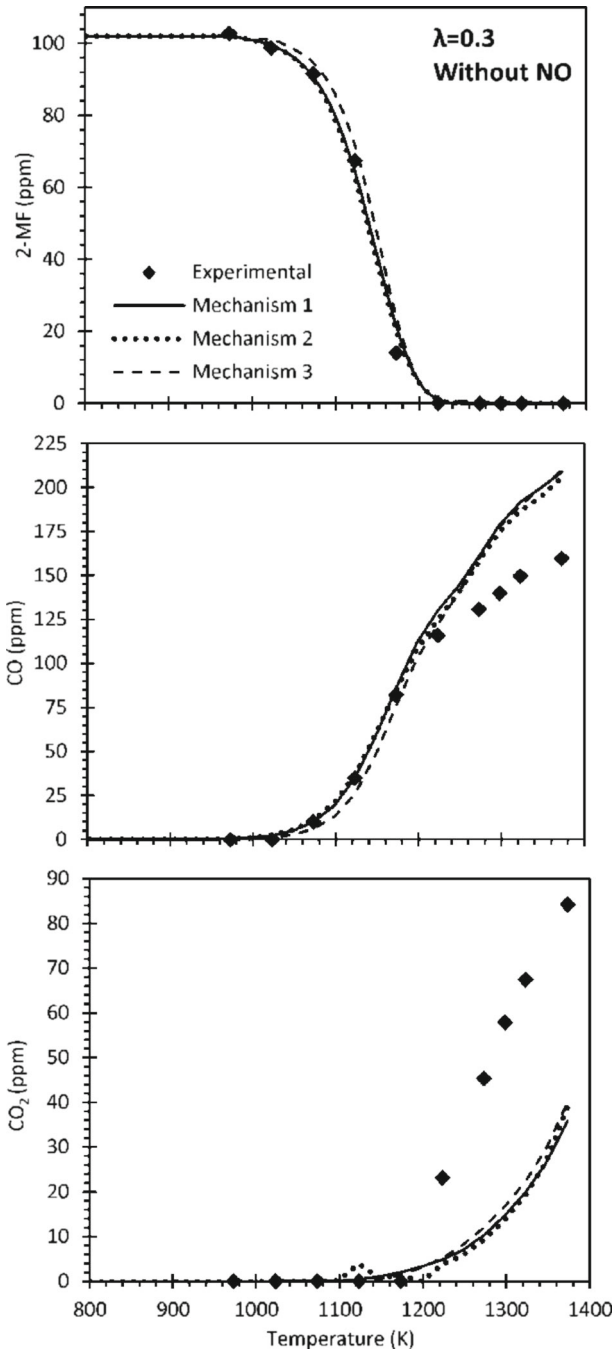
Fig. 1 Concentration profiles of 2-MF, CO, and CO$_2$, as a function of temperature, in the 2-MF oxidation in the absence of NO for $\lambda = 0.3$, at atmospheric pressure. Symbols: experimental results. Solid line: mechanism 1, dotted line: mechanism 2, dashed line: mechanism 3
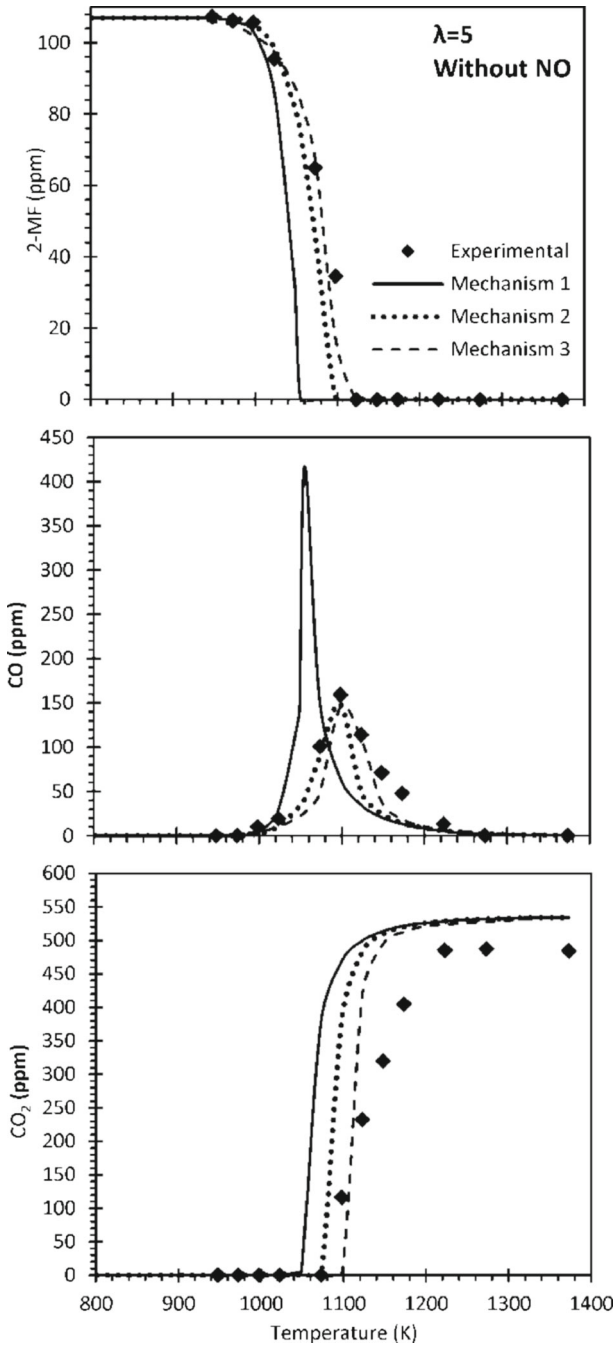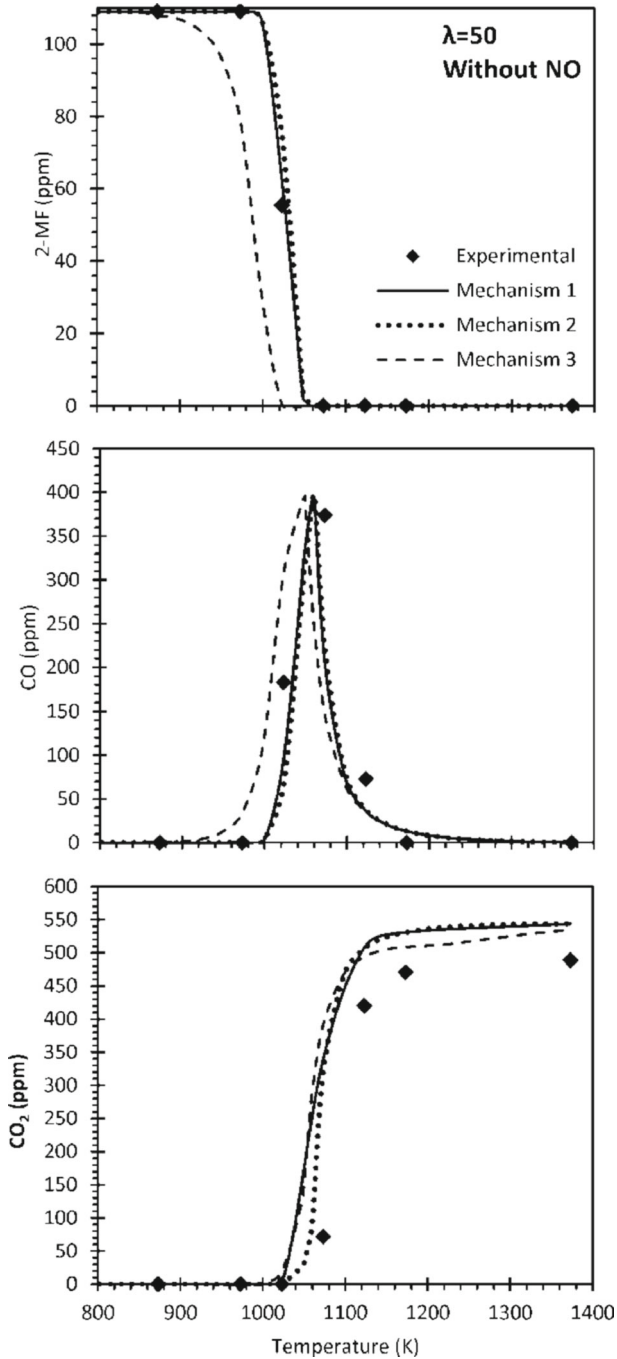
Fig. 2 Concentration profiles of 2-MF, CO, and CO$_2$, as a function of temperature, in the 2-MF oxidation in the absence of NO for $\lambda = 5$, at atmospheric pressure. Symbols: experimental results. Solid line: mechanism 1, dotted line: mechanism 2, dashed line: mechanism 3

Fig. 3 Concentration profiles of 2-MF, CO, and CO_2, as a function of temperature, in the 2-MF oxidation in the absence of NO for $\lambda = 50$, at atmospheric pressure. Symbols: experimental results. Solid line: mechanism 1, dotted line: mechanism 2, dashed line: mechanism 3

4 Results and Discussion

Experiments of 2-MF oxidation in the absence and presence of NO have been performed in a flow reactor. In this way, the influence of the oxygen concentration and the presence of NO on the 2-MF oxidation, as well as, the 2-MF capacity to reduce the NO concentration for different oxygen concentrations, have been studied. A detailed kinetic model, including the mechanism progressively develop in our group, together with the reaction sub-mechanism for 2-MF by Somers et al. [20] has been selected to simulate the experimental results. The main reaction pathways of 2-MF and NO consumption under the different conditions studied are identified through modelling calculations.

Figures 4 and 5 show experimental data and modelling predictions for the 2-MF oxidation in the absence and presence of NO as a function of temperature, for the different λ values studied, ranging from 0.3 to 50. The figures include concentration results of 2-MF and H_2 (left part of the figures), the latter when applicable, and of CO and CO_2 (right part of the figures). As discussed in the previous section, in general, the model agrees well with the experimental data obtained. However, some discrepancies between experimental results and modelling calculations are found, with the major discrepancies for $\lambda =5$ in the presence of NO, and for $\lambda = 50$ in the absence of NO (Fig. 5).

Regarding the influence of oxygen concentration on the 2-MF consumption, it is observed that under very fuel-rich ($\lambda = 0.3$) and stoichiometric conditions ($\lambda =1$), and both in the absence and in the presence of NO (Fig. 4), the oxygen concentration does not influence the onset of 2-MF consumption, thus 2-MF begins to be consumed approximately at
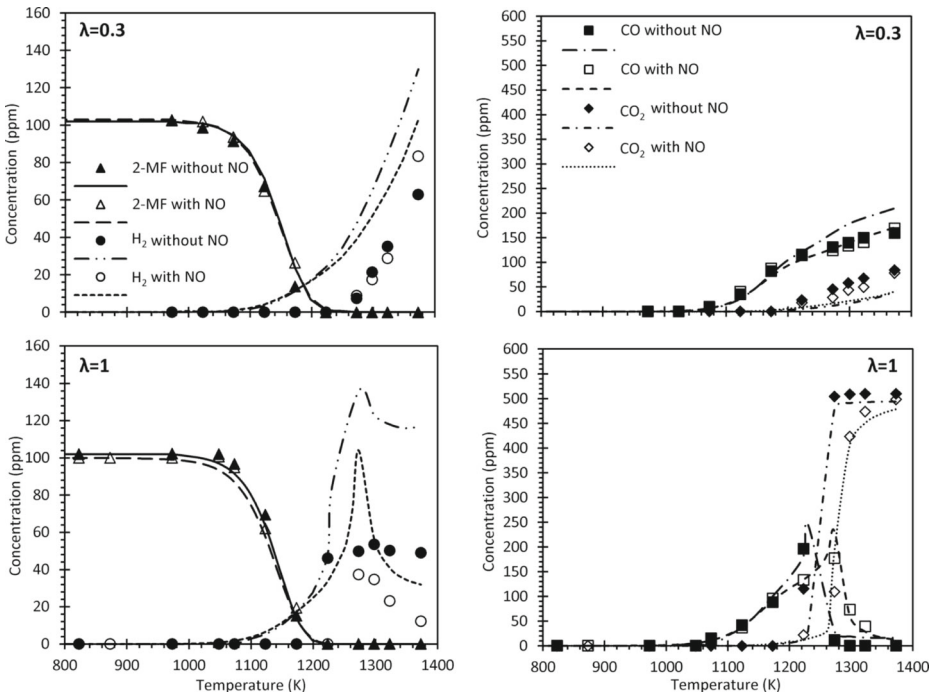

Fig. 4 Concentration profiles of the major species, as a function of temperature, in the 2-MF oxidation for $\lambda = 0.3$ and 1, at atmospheric pressure. Experimental data (symbols) and modelling predictions (lines)
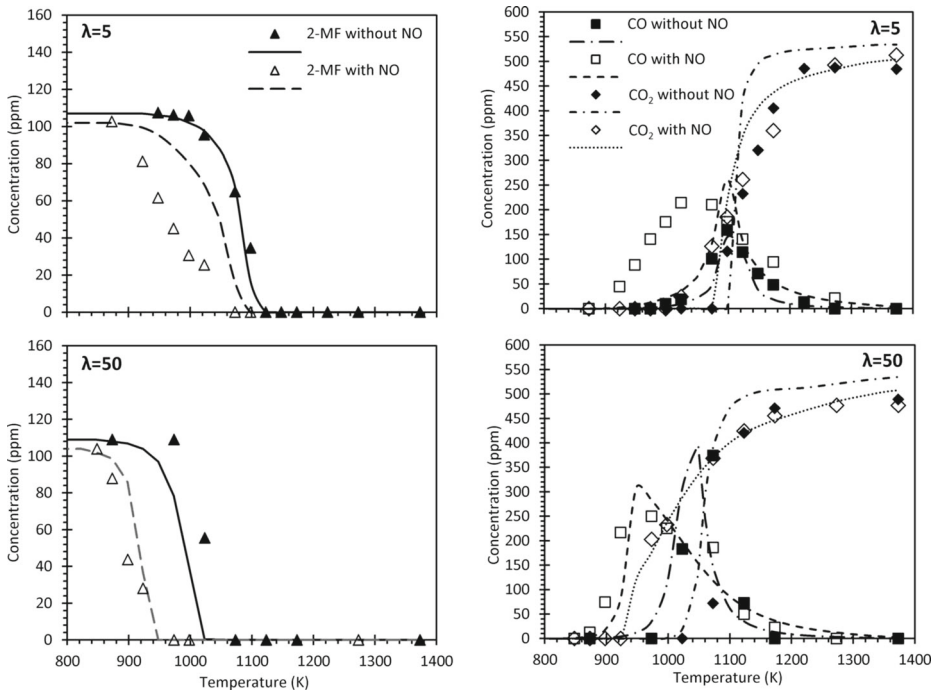
Fig. 5 Concentration profiles of the major species, as a function of temperature, in the 2-MF oxidation for $\lambda =5$ and 50, at atmospheric pressure. Experimental data (symbols) and modelling predictions (lines)

1050 K. However, under fuel-lean ($\lambda = 5$) and very fuel-lean ($\lambda = 50$) conditions (Fig. 5), and both in the absence and in the presence of NO, the onset of 2-MF consumption is shifted toward lower temperatures with the increasing of the oxygen concentration.
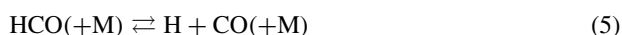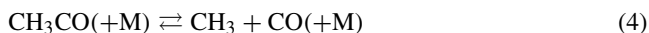
The concentration profile of 2-MF is also influenced by the presence of NO for $\lambda = 5$ and 50 (Fig. 5). In this way, the onset of 2-MF consumption is shifted to lower temperatures in the presence of NO, as it was observed earlier for other oxygenated compounds [33, 34, 36]. It can be due to the fact that the formation of OH radicals is promoted under these conditions, which will be analyzed later. On the other hand, for $\lambda = 0.3$ and 1 (Fig. 4) no appreciable influence of the NO presence on the onset of 2-MF consumption can be observed. It could be attributed to the fact that under very fuel-rich and stoichiometric conditions, the thermal decomposition of 2-MF is a very important path for its consumption.

The onset for 2-MF consumption is accompanied by the formation of H_2 and CO. H_2 is formed only under very fuel-rich and stoichiometric conditions (Fig. 4). For both conditions, the model overestimates the H_2 concentration and it is observed that NO acts to diminish the H_2 formation with the increasing of temperature. For $\lambda = 0.3$, the H_2 concentration increases with the increase of temperature, while for $\lambda = 1$, a maximum in the H_2 concentration is reached. In this case, H_2 is consumed to give water and H radicals, through the reaction (1).

$$OH + H_2 \leftrightarrows H_2O + H \qquad (1)$$

CO is formed for all the λ values studied, and, except for $\lambda = 0.3$, a maximum in the concentration profile of CO is reached, which is shifted to lower temperatures as the oxygen concentration increases (Figs. 4 and 5). For $\lambda = 0.3$ and 1 (Fig. 4), the presence of NO does

not influence the onset of formation of CO, but influences the CO concentration formed at the higher temperatures studied. According to simulations, at intermediate temperatures (when still the influence of NO is not observed), and both in the absence and in the presence of NO, CO is formed through the following reactions:

$$CH_2CHCHCHCO \rightleftarrows CHCHCHCH_2 + CO \tag{2}$$

$$CH_3CHCCHCHO \rightleftarrows CHCCH_2CH_3 \quad + CO \tag{3}$$

$$CH_3CO(+M) \rightleftarrows CH_3 + CO(+M) \tag{4}$$

$$HCO(+M) \rightleftarrows H + CO(+M) \tag{5}$$

However, for the higher temperatures and in the absence of NO, the major routes to the formation of CO are the reactions (5) and 6,

$$HCCO + O_2 \rightleftarrows 2CO + OH \tag{6}$$

while in the presence of NO, the formation of CO for the higher temperatures occurs only through the reaction (5), because the HCCO radicals, instead of reacting to form CO (reaction (6)), react with NO to form HCN and, with minor importance, HCNO through the reactions (7) and (8), respectively. In this way, with the increase of temperature, the presence of NO diminishes the CO concentration formed, and shifts the maximum concentration of CO to higher temperatures for stoichiometric conditions.

$$HCCO + NO \rightleftarrows HCN + CO_2 \tag{7}$$

$$HCCO + NO \rightleftarrows HCNO + CO \tag{8}$$
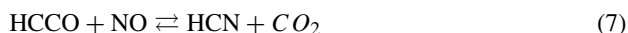
For $\lambda = 5$ and 50 (Fig. 5), the presence of NO modifies the onset of formation of CO, by shifting the onset of the consumption of 2-MF toward lower temperatures.

CO_2 is formed for all the λ values studied, both in the absence and in the presence of NO, and its concentration increases with increasing temperature. For $\lambda = 1, 5$, and 50, the beginning of formation of CO_2 coincides with the maximum of the CO concentration profile. Under these conditions, 2-MF is completely oxidized to CO_2 at the highest temperature studied, whereas for $\lambda = 0.3$, the lack of oxygen prevents complete oxidation of 2-MF.

Minor species, such as C_2H_4 and C_2H_2, were found in the experiments performed under very fuel-rich conditions. The concentration profiles of these species as a function of temperature are shown in Fig. 6. The C_2H_4 concentration profile shows a maximum, while with increasing temperature, increases C_2H_2 concentration. The model predicts the trend of experimental results for both C_2H_4 and C_2H_2, but does not fit well to them. The model underestimates the maximum concentration of C_2H_4, although for both experimental and modelling data, C_2H_4 peaks around 1273 K. On the other hand, the model overestimates the C_2H_2 concentration.

Figure 7 shows the rate of production analysis at 50 % 2-MF consumption for both in the absence and in the presence of NO. When NO is present, no appreciable differences have been found for the 2-MF reaction routes. However, NO is found to act by modifying the radical pool and thus favoring certain reactions over others.

Under very fuel-rich and stoichiometric conditions, the thermal decomposition of 2-MF involving carbene intermediates occurs to form 1-butyne ($CHCCH_2CH_3$) and CO (pathway 1), or, only under very fuel-rich conditions, to form propargyl (H_2CCCH) and acetyl (CH_3CO) radicals (pathway 2).

From $\lambda = 0.3$ to $\lambda = 5$, the H-atom addition occurs at the C5 site of 2-MF to ultimately form vinyl ketene ($CH_2CHCHCO$) and methyl radicals (pathway 3). $CH_2CHCHCO$ formed can be consumed by different reactions involving the H/O radical pool, depending on the
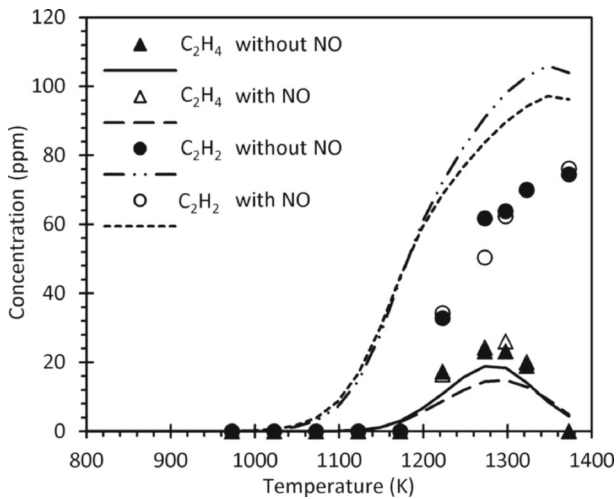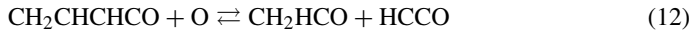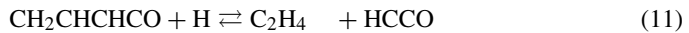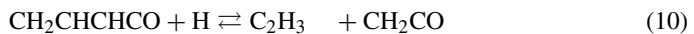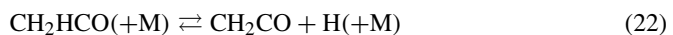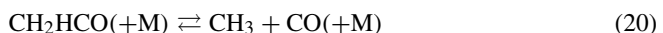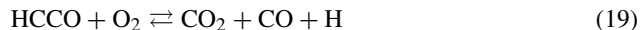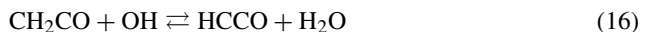
Fig. 6 Concentration profiles of the minor species, as a function of temperature, in the 2-MF oxidation for $\lambda = 0.3$, at atmospheric pressure. Experimental data (symbols) and modelling predictions (lines)

oxygen present in the environment to give as principal path the formation of 2-methyl vinyl radical (CH$_3$CHCH) and CO (reaction (9)), and with minor importance the formation of ketene (CH$_2$CO), and ketenyl (HCCO) and CH$_2$HCO radicals (reactions(10-13)),

$$CH_2CHCHCO + H \rightleftarrows CH_3CHCH + CO \quad (9)$$

$$CH_2CHCHCO + H \rightleftarrows C_2H_3 \quad + CH_2CO \quad (10)$$

$$CH_2CHCHCO + H \rightleftarrows C_2H_4 \quad + HCCO \quad (11)$$

$$CH_2CHCHCO + O \rightleftarrows CH_2HCO + HCCO \quad (12)$$

$$CH_2CHCHCO + O \rightleftarrows 2CH_2CO \quad (13)$$

Under very fuel-rich and stoichiometric conditions, CH$_2$CHCHCO is consumed through its reaction with H radicals, i.e, reactions (9-11). However, as the stoichiometry becomes leaner ($\lambda = 5$), CH$_2$CHCHCO, in addition to react with H radicals, also reacts with O radicals through reactions (12) and (13). Later, and depending on the oxygen available and on the presence of NO, ketene and HCCO radicals react with the H/OH radical pool and molecular oxygen, respectively, being oxidized to CO and CO$_2$ (reactions (14-19)), while CH$_2$HCO radicals decompose thermally (reactions (20-22)),

$$CH_2CO + H \rightleftarrows CH_3 + CO \quad (14)$$

$$CH_2CO + OH \rightleftarrows CH_2OH + CO \quad (15)$$

$$CH_2CO + OH \rightleftarrows HCCO + H_2O \quad (16)$$

$$CH_2CO + OH \rightleftarrows CH_3 \quad + CO_2 \quad (17)$$

$$HCCO + O_2 \rightleftarrows 2CO + OH \quad (18)$$

$$HCCO + O_2 \rightleftarrows CO_2 + CO + H \quad (19)$$

$$CH_2HCO(+M) \rightleftarrows CH_3 + CO(+M) \quad (20)$$

$$CH_2HCO \rightleftarrows CH_3 + CO \quad (21)$$

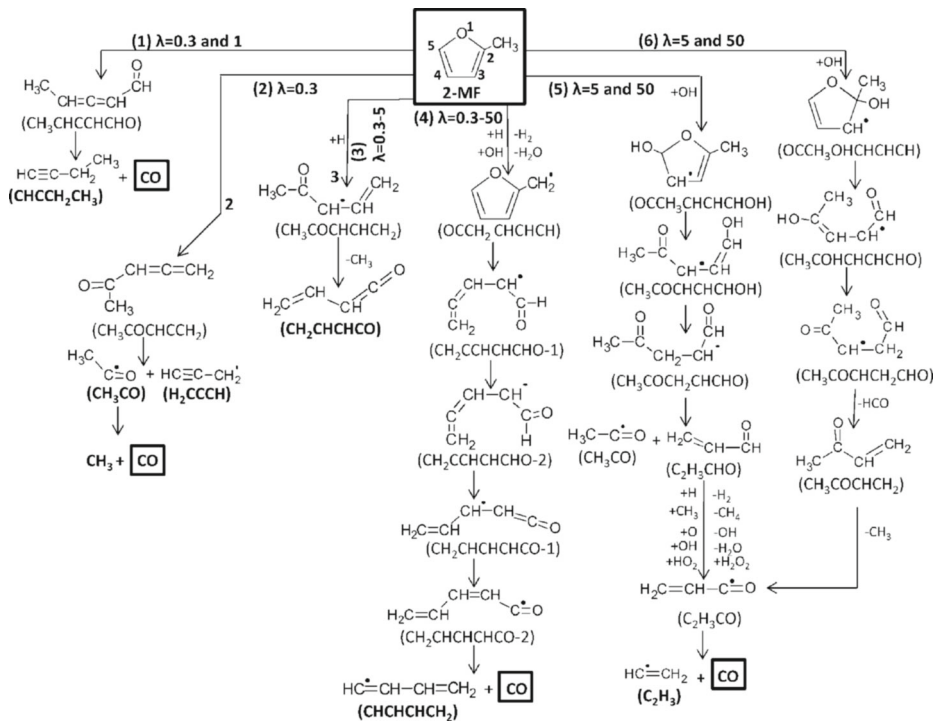$$CH_2HCO(+M) \rightleftarrows CH_2CO + H(+M) \quad (22)$$

Fig. 7 Rate of production analysis for 2-MF oxidation both in the absence and in the presence of NO, carried out under at approximately 50 % 2-MF consumption

Ketene consumption occurs in the same way both in the absence and in the presence of NO, but is affected by the availability of oxygen. Under stoichiometric and fuel-lean conditions, the ketene consumption occurs through (14-17) reactions, while under very fuel-rich conditions, the ketene consumption occurs only through r14 and r15 reactions. Regarding the HCCO consumption, it occurs in one way or another depending on whether NO is present or not. In the absence of NO, HCCO reacts with molecular oxygen (reactions (18) and 19)) for all the stoichiometries studied, but when NO is present, HCCO also interacts with NO. Then, in the presence of NO, for very fuel-rich and stoichiometric conditions, HCCO consumption is no longer given by reactions (18) and (19), but instead HCCO reacts with NO mainly through reactions (7) and (8). On the other hand, under fuel-lean conditions, the increase in oxygen concentration allows HCCO to interact both with NO and molecular oxygen (reactions (7), (8), (18) and (19)). Finally, CH_2HCO radicals, which are formed only under fuel-lean ($\lambda = 5$) conditions as it has been mentioned earlier, are consumed by thermal decomposition (reactions (20-22)) both in the absence and in the presence of NO.

For all λ values, $\lambda = 0.3 - 50$, the H-abstraction from the methyl group of 2-MF by H (principally for $\lambda = 0.3$ and 1) and OH radicals (principally for $\lambda = 5$ and 50) (pathway 4) to give as an intermediate product the resonance-stabilized 2-methylfuranyl radicals ($OCCH_2CHCHCH$) occurs. Thus, ring opening via cleavage of the C-O bond results to finally yield n-butadienyl radicals ($CHCHCHCH_2$) and CO. The $CHCHCHCH_2$ radicals formed by this path react with oxygen (reaction (23)) promoting the formation of HO_2 radicals (reaction (24)), which are involved in the NO-NO_2 interconversion (reactions (25) and
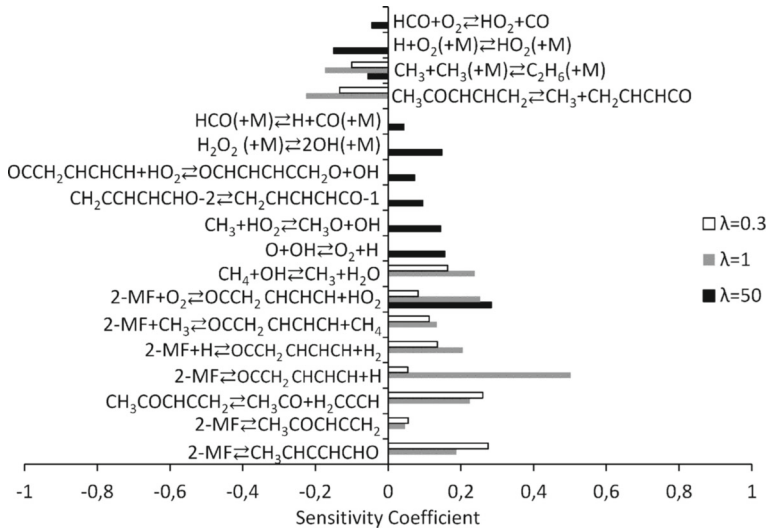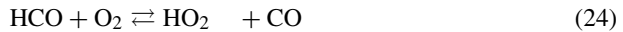
Fig. 8 Sensitivity analysis for 2-MF oxidation in the absence of NO (sets 1, 3, and 7 in Table 1, at 1048, 1048, and 923 K, respectively)

(26)) resulting in an increase of OH radicals production, which are the main responsible for 2-MF consumption under fuel-lean and very fuel-lean conditions. Because of this, in the presence of NO and for $\lambda = 5$ and 50, the 2-MF oxidation beings to occur at lower temperatures as the stoichiometry becomes leaner, as can be seen in Fig. 5.

$$CHCHCHCH_2 + O_2 \rightleftarrows C_2H_3CHO + HCO \tag{23}$$

$$HCO + O_2 \rightleftarrows HO_2 \quad + CO \tag{24}$$

$$NO + HO_2 \rightleftarrows NO_2 \quad + OH \tag{25}$$

$$NO_2 \quad + H \rightleftarrows NO + OH \tag{26}$$

Other important paths for the 2-MF consumption, for $\lambda = 5$ and 50, are the OH-addition at the C5 (pathway 5) and at the C2 (pathway 6) sites of 2-MF to form acroleine (C_2H_3CHO) and methyl vinyl ketone ($CH_3COCHCH_2$), respectively, both products culminating in the formation of vinyl radicals (C_2H_3) and CO. The OH-addition process has been mentioned by Wei et al. [14] as reactions that contribute very little to 2-MF consumption, while in the work of Uygun et al. [15] it is mentioned that 2-MF is mainly consumed by the OH-addition at C5 and at C2 sites of 2-MF under their experimental conditions.

The H-addition at the C2 site of 2-MF to form furan and methyl radicals has been identified in the work of Tran et al. [22] as an important path for the consumption of 2-MF. However, in the rate of production analysis made in Fig. 7, this path does not appear as a principal path for the 2-MF consumption. This could be due to the fact that the sub-mechanism for 2-MF from Somers et al. [20] used in the present calculations includes the reaction of the H-addition at the C5 site of 2-MF to lead to the formation of vinyl ketene ($CH_2CHCHCO$), which has been detected experimentally in the work of Moshammer et al. [26] on the combustion chemistry of 2-MF.

Figures 8 and 9 present sensitivity coefficients obtained through a first-order sensitivity analysis of CO at the temperature at which 2-MF starts to be consumed for both in the absence (sets 1, 3 and 7 in Table 1) and in the presence of NO (sets 2, 4 and 8 in Table 1),

respectively. The sensitivity coefficients are calculated as $S = \delta Y_j/\delta A_i$, where Y_j is the mass fraction of the jth species and A_i is the pre-exponential constant for reaction i [38]. Positive coefficients correspond to reactions which promote reactivity and vice versa.

It can be seen in Figs. 8 and 9 that the reactions to which the 2-MF conversion is more sensitive depend on the oxygen concentration and on the presence of NO. Both in the absence and in the presence of NO, the 2-MF conversion is more sensitive to the reactions involving the 2-MF thermal decomposition and the thermal decomposition of its intermediates ($CH_3COCHCCH_2$, $CH_2CCHCHCHO$-2, and $CH_3COCHCHCH_2$). Another important reaction in the conversion process of 2-MF, both in the absence and in the presence of NO, is the H-abstraction from the methyl side (C2 site) in 2-MF by small species (H and O_2) to give the 2-methylfuranyl radical ($OCCH_2CHCHCH$). The chain-branching reaction (27),

$$O + OH \rightleftarrows O_2 + H \tag{27}$$

also appears to influence the 2-MF conversion, both in the absence and in the presence of NO. The interactions between methane with OH radicals, molecular oxygen with H radicals, and the reaction of recombination of methyl radicals also appear to be important.

In the absence of NO, other reactions to which the 2-MF conversion is sensitive include: 1) the 2-MF interaction with methyl radicals, 2) the reaction between 2-methylfuranyl radicals and HO_2, and 3) the formation of HO_2, and H and OH radicals through reactions (5), (24) and those involving the hydrogen peroxide decomposition, and the interaction of methyl radicals with HO_2.

On the other hand, in the presence of NO, the reactions: 1) H-abstraction from the methyl side in 2-MF by OH radicals, and 2) methyl radicals with NO, also appear to be important for the 2-MF conversion. Furthermore, the decomposition of the $CH_3COCHCHCHOH$, and $CH_3COHCHCHCHO$ intermediates appear also as sensitive reactions.
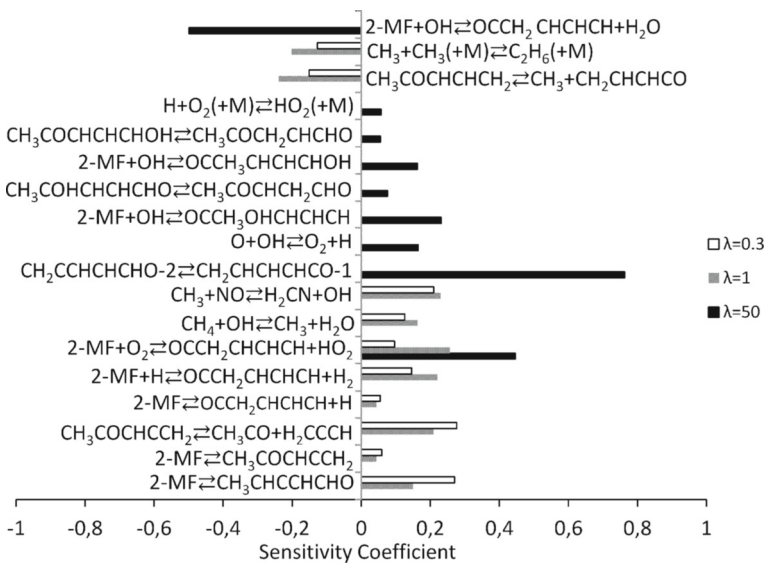

Fig. 9 Sensitivity analysis for 2-MF oxidation in the presence of NO (sets 2, 4, and 8 in Table 1, at 1048, 1048, and 873 K, respectively)

Having analyzed the influence of the oxygen concentration and the presence of NO on the 2-MF oxidation, the capacity of 2-MF to reduce the NO concentration in the different environments studied will be now discussed. Figure 10 shows the experimental data and the modelling calculations of the NO concentration profile as a function of temperature for all λ values studied. For $\lambda = 0.3$ and 1 (upper part of the Fig. 10), it is seen that with the increase of temperature, the NO concentration decreases slightly, while for $\lambda = 5$ and 50 (lower part of the Fig. 10), a minimum in the NO concentration profile is observed, which is more noticeable for $\lambda = 50$.

Figure 11 shows the reaction path diagram for the NO consumption. For $\lambda = 0.3$ and 1, the reaction of NO with C_2H_3 radicals to give HNO is an important via for the NO consumption. Also, the reaction of NO with HCCO radicals to give HCN (reaction (7)), and with CH_3 radicals, to give HCN and H_2CN, are important routes for the NO consumption.
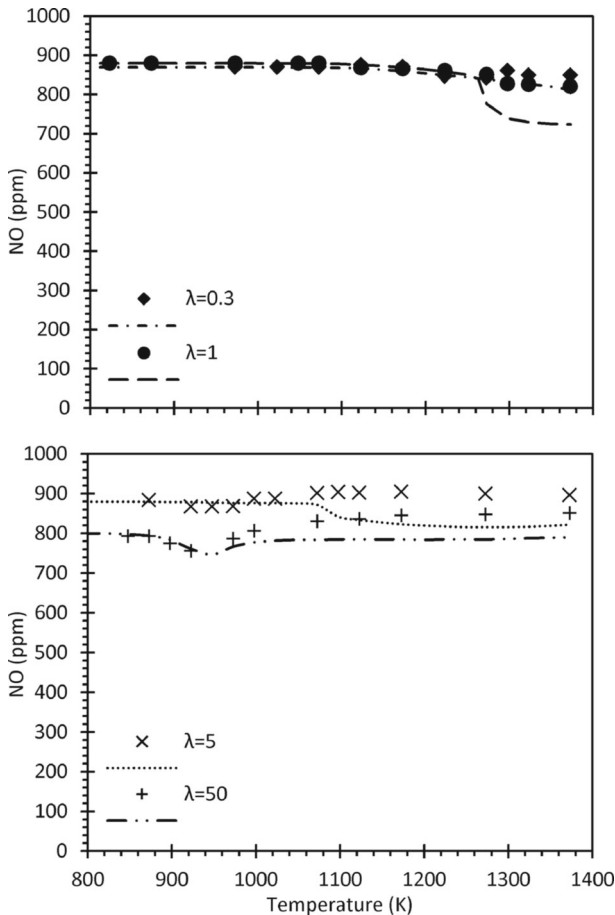

Fig. 10 Concentration profile of NO, as a function of temperature, for $\lambda = 0.3$, 1 (top), 5 and 50 (bottom), at atmospheric pressure. Experimental data (symbols) and modelling predictions (lines)

Besides these paths, another route for NO consumption, from stoichiometric to very fuel-lean conditions, is the reaction of NO with HO_2 to give NO_2 and OH radicals. Also, under fuel-lean and very fuel-lean conditions the reaction between NO and CH_3O_2 radicals to give NO_2 can occur.

For both $\lambda = 0.3$ and 1, the main path for NO consumption involves the sequence: $NO \rightarrow HCN \rightarrow CH_3CN \rightarrow CH_2CN \rightarrow CN \rightarrow NCO \rightarrow N_2/N_2O$. For $\lambda = 0.3$ and 1, N_2O forms NO by reaction with H radicals, and for $\lambda = 0.3$ also N_2O decomposes to N_2. However, for $\lambda = 0.3$ and 1, the main path for the consumption of NCO is its reaction with NO to give N_2. In this way, under very fuel-rich and stoichiometric conditions, NO is reduced basically by reburn reactions [27, 39].

With the increase of the oxygen concentration ($\lambda = 5$ and 50), the most important reaction for NO consumption is the reaction of NO with HO_2 to form NO_2 and OH radicals (reaction (25)). In this way, the minimum observed in the Fig. 10 could be due to the NO-NO_2 interconversion which occurs through the reaction of NO_2 with CH_3 and H radicals to give back NO. This interconversion limits a net reduction of NO.

The mechanism compiled in this work has also been used to simulate the ignition delay times measured by Wei et al. [14]. As an example, Fig. 12 shows the experimental and modelling calculation results for the operating conditions: $\varphi = 1$, 2-MF=1 %, $O_2 = 6$, Ar=93 %, P=1.25, 4.25, and 10.65 bar. The simulations for other conditions can be seen in Figs. S8-S12 in Online Resource. Results obtained reveal that the mechanism captures also with good accuracy the ignition behavior of 2-MF for the different mixtures and the different pressures evaluated.
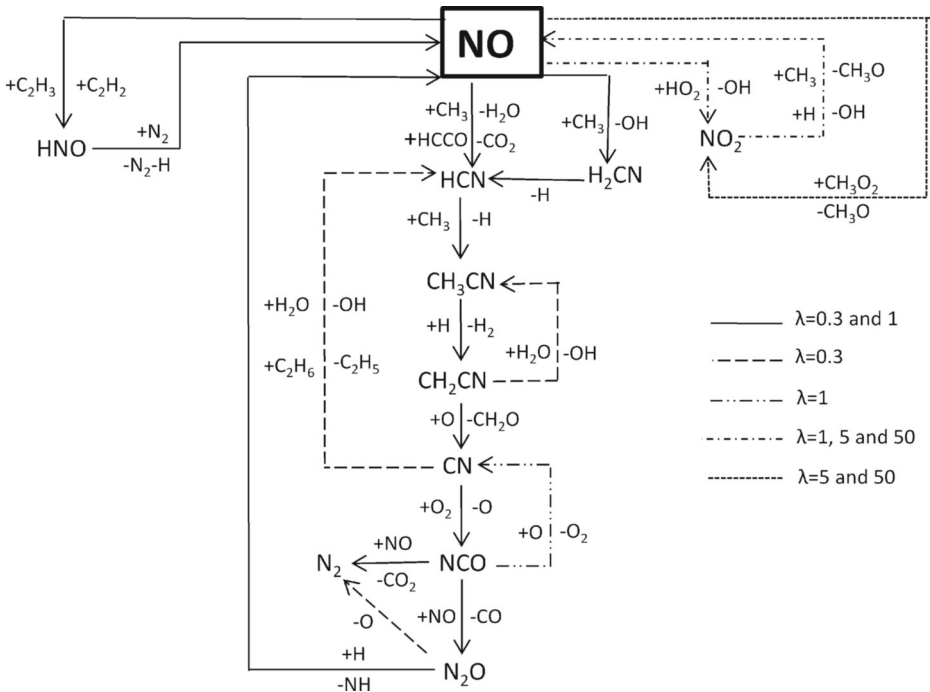

Fig. 11 Reaction path diagram for the NO consumption, for $\lambda = 0.3$, 1, 5 and 50
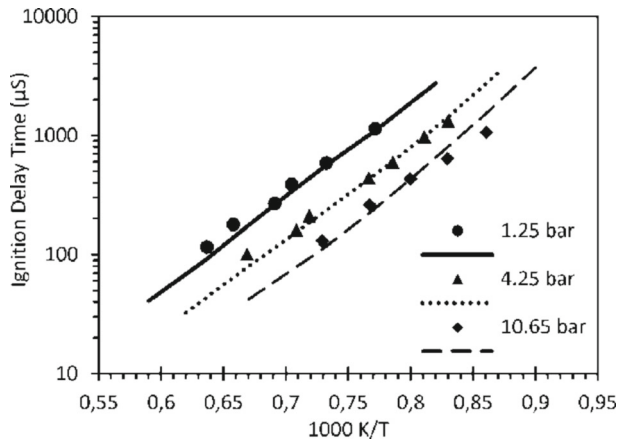
Fig. 12 Experimental ignition delay times (symbols) and modelling predictions (lines), for $\varphi = 1$ ($\lambda = 1$), 2-MF=1 %, $O_2 = 6$ %, Ar=93 %, at 1.25, 4.25, and 10.65 bar

5 Conclusions

A study of 2-methylfuran oxidation has been performed in a flow reactor installation at different temperatures and air excess ratio values. The experiments have been also performed in the presence of 900 ppm of NO. In this way, the influence of the stoichiometry, and the presence of NO on the 2-MF oxidation, as well as the capacity of 2-MF to reduce the NO concentration at different stoichiometries, have been studied. Modelling calculations using three different reaction sub-mechanisms for 2-MF conversion incorporated to a base model, have been compared with the experimental data. In general, the three sub-mechanisms for 2-MF conversion reproduce reasonably well the experimental trends, but best results begin observed using the mechanism that incorporates the 2-MF sub-mechanism by Somers et al. [20], even though this model fails to predict the experimental data for $\lambda = 5$ in the presence of NO, and for $\lambda = 50$ in the absence of NO.

The results of performing both, rate of production and sensitivity analysis indicate that: 1) for very fuel-rich and stoichiometric conditions, the temperature for the onset for the conversion of 2-MF remains the same because the thermal decomposition of 2-MF appears to be the main conversion pathway. On the other hand, under fuel-lean and very fuel-lean conditions, the onset for the 2-MF consumption is shifted to lower temperatures as the oxygen concentration increases, because its reaction with OH radicals appears to be the main responsible for the 2-MF consumption, 2) the 2-MF reaction routes appear to be the same, for both in the absence and in the presence of NO. However, NO is found to act by modifying the radical pool and thus favors certain reactions over others. Thus, for fuel-lean and very fuel-lean conditions, when NO is present, the displacement of the onset for the 2-MF consumption to lower temperatures is greater because the formation of OH radicals is more favored than in the absence of NO, 3) under very fuel-rich and stoichiometric conditions the presence of NO does not affect the onset of formation products as CO, but diminishes the concentration at higher temperatures due to the occurrence of competing reactions, and 4) when NO is added, it is converted to N_2 by reaction with HCCO and CH_3 radicals (reburn reactions) under very fuel-rich and stoichiometric conditions, while under fuel-lean and very-fuel lean conditions, the NO-NO_2 interconversion is the dominant step.

Compliance to Ethical Standard   This manuscript has not been published and is not under consideration for publication elsewhere. However, this same manuscript, with some additional changes, was presented in the SPEIC2014 meeting, held in Lisbon, from 19-21 November 2014. The organizing committee of this meeting offered us to submit this manuscript to the SPEIC2014 Special Issue of Flow, Turbulence and Combustion.

Consent to submit the manuscript has been received from all co-authors. We have no conflicts of interest to disclose.

References

1. Román-Leshkov, Y., Barret, C.J., Liu, Z.Y., Dumesic, J.A.: Production of dimethylfuran for liquid fuels from biomass-derived carbohydrates. Nature **447**, 982–985 (2007)
2. Zhao, H., Holladay, J.E., Brown, H., Zhang, Z.C.: Metal chlorides in ionic liquid solvents convert sugars to 5-hydroxymethylfurfural. Science **316**, 1597–1600 (2007)
3. Mascal, M., Nikitin, E.B.: Direct high-yield conversion of cellulose into biofuel. Angew. Chem. **47**, 7924–7926 (2008)
4. Alexandrino, K., Millera, A., Bilbao, R., Alzueta, M.U.: Interaction between 2,5-dimethylfuran and nitric oxide: experimental and modeling study. Energy Fuels **28**, 4193–4198 (2014)
5. Alexandrino, K., Millera, A., Bilbao, R., Alzueta, M.U.: Novel aspects in the pyrolysis and oxidation of 2,5-dimethylfuran. Proc. Combust. Inst. **35**, 1717–1725 (2015)
6. Thewes, M., Muether, M., Pischinger, S., Budde, M., Brunn, A., Sehr, A., Adomeit, P., Klankermayer, J.: Analysis of the impact of 2-methylfuran on mixture formation and combustion in a direct-injection spark-iginition engine. Energy Fuels **25**, 5549–5561 (2011)
7. Pan, M., Shu, G., Pan, J., Wei, H., Feng, D., Guo, Y., Liang, Y.: Performance comparison of 2-methylfuran and gasoline on a spark-ignition engine with cooled exhaust gas recirculation. Fuel **132**, 36–43 (2014)
8. Wang, C., Xu, H., Daniel, R., Ghafourian, A., Herreros, J.M., Shuai, S., Ma, X.: Combustion characteristics and emissions of 2-methylfuran compared to 2,5-dimethylfuran, gasoline and ethanol in a DISI engine. Fuel **103**, 200–211 (2013)
9. Grela, M.A., Amorebieta, V.T., Colussi, A.J.: Very low pressure pyrolysis of furan, 2-methylfuran, and 2,5-dimethylfuran. The stability of the furan ring. J. Phys. Chem. **89**, 38–41 (1985)
10. Lifshitz, A., Tamburu, C., Shashua, R.: Decomposition of 2-methylfuran. Experimental and modeling study. J. Phys. Chem. A **101**, 1018–1029 (1997)
11. Wei, L., Li, Z., Tong, L., Wang, Z., Jin, H., Yao, M., Zheng, Z., Wang, C., Xu, H.: Primary combustion intermediates in lean and rich low-pressure premixed laminar 2-methylfuran/oxygen/argon flames. Energy Fuels **26**, 6651–6660 (2012)
12. Ma, X., Jiang, C., Xu, H., Shuai, S., Ding, H.: Laminar burning characteristics of 2-methylfuran compared with 2,5-dimethylfuran and isooctane. Energy Fuels **27**, 6212–6221 (2013)
13. Ma, X., Jiang, C., Xu, H., Ding, H., Shuai, S.: Laminar burning characteristics of 2-methylfuran and isooctane blend fuels. Fuel **116**, 281–291 (2014)
14. Wei, L., Tang, C., Man, X., Huang, Z.: Shock-tube experiments and kinetic modeling of 2-methylfuran ignition at elevated pressure. Energy Fuels **27**, 7809–7816 (2013)
15. Uygun, Y., Ishihara, S., Olivier, H.: A high pressure ignition delay time study of 2-methylfuran and tetrahydrofuran in shock tubes. Combust. Flame **161**, 2519–2530 (2014)
16. Eldeeb, M.A., Akih-Kumgeh, B.: Reactivity trends in furan and alkyl furan combustion. Energy Fuels **28**, 6618–6626 (2014)
17. Xu, N., Tang, C., Meng, X., Fan, X., Tian, Z., Huang, Z.: Experimental and kinetic study on the ignition delay times of 2,5-dimethylfuran and the comparison to 2-methylfuran and furan, Energy Fuels, doi:10.1021/acs.energyfuels.5b00906 (2015)
18. Davis, A.C., Sarathy, S.M.: Computational study of the combustion and atmospheric decomposition of 2-methylfuran. J. Phys. Chem. A **117**, 7670–7685 (2013)
19. Somers, K.P., Simmie, J.M., Gillespie, F., Burke, U., Connolly, J., Metcalfe, W.K., Battin-Leclerc, F., Dirrenberger, P., Herbinet, O., Glaude, P.-A., Curran, H.J.: A high temperature and atmospheric pressure

experimental and detailed chemical kinetic modelling study of 2-methyl furan oxidation. Proc. Combust. Inst. **34**, 225–232 (2013)

20. Somers, K., Simmie, J., Metcalfe, W., Curran, H.: The pyrolysis of 2-MF: a quantum chemical, statistical rate theory and kinetic modeling study. Phys. Chem. Chem. Phys. **16**, 5349–5367 (2014)

21. Liu, D., Togbé, C., Tran, L.S., Felsmann, D., Oßwald, P., Nau, P., Koppmann, J., Lackner, A., Glaude, P.A., Sirjean, B., Fournet, R., Battin-Leclerc, F., Kohse-Höinghaus, K.: Combustion chemistry and flame structure of furan group using molecular-beam mass spectrometry and gas chromatography–Part I: Furan. Combust. Flame **161**, 748–765 (2014)

22. Tran, L.S., Togbé, C., Liu, D., Felsmann, D., Oßwald, P., Glaude, P.-A., Fournet, R., Sirjean, B., Battin-Leclerc, F., Kohse-Höinghaus, K.: Combustion chemistry and ?ame structure of furan group biofuels using molecular-beam mass spectrometry and gas chromatography–Part II: 2-methylfuran. Combust. Flame **161**, 766–779 (2014)

23. Togbé, C., Tran, L.S., Liu, D., Felsmann, D., Oßwald, P., Glaude, P.A., Sirjean, B., Fournet, R., Battin-Leclerc, F., Kohse-Höinghaus, K.: Combustion chemistry and flame structure of furan group using molecular-beam mass spectrometry and gas chromatography–Part III: 2,5-dimethylfuran. Combust. Flame **161**, 780–797 (2014)

24. Sirjean, B., Fournet, R., Glaude, P.A., Battin-Leclerc, F., Wang, W., Oehlschlaeger, M.A.: Shock tube and chemical kinetic modeling study of the oxidation of 2,5-dimethylfuran. J. Phys. Chem. A. **117**, 1371–1392 (2013)

25. Tian, Z., Yuan, T., Fournet, R., Glaude, P.A., Sirjean, B., Battin-Leclerc, F., Zhang, K., Qi, F.: An experimental and kinetic investigation of premixed furan/oxygen/flames. Combust. Flame **158**, 756–773 (2011)

26. Moshammer, K., Lucassen, A., Togbé, C., Kohse-Höinghaus, K., Hansen, N.: Formation of oxygenated and hydrocarbon intermediates in premixed combustion of 2-methylfuran. Z. Phys. Chem. **229**, 507–528 (2015)

27. Glarborg, P., Alzueta, M.U., Dam-Johansen, K., Miller, J.A.: Kinetic modeling of hydrocarbon nitric oxide interactions in a flow reactor. Combust. Flame **115**, 1–27 (1998)

28. Abián, M., Silva, S.L., Millera, A., Bilbao, R., Alzueta, M.U.: Effect of operating conditions on NO reduction by acetylene-ethanol mixtures. Fuel Process Technol. **91**, 1204–1211 (2010)

29. Kristensen, P.G., Glarborg, P., Dam-Johansen, K.: Nitrogen chemistry during burnout in fuel-staged combustion. Combust. Flame **107**, 211–222 (1996)

30. Yanfeng, G., Shenghua, L., Hejun, G., Tiegang, H., Longbao, Z.: A new diesel oxygenate additive and its effects on engine combustion and emissions. Appl. Therm. Eng. **27**, 202–207 (2007)

31. Yao, C., Cheung, C.S., Cheng, C., Wang, Y., Chan, T.L., Lee, S.C.: Effect of Diesel/methanol compound combustion on Diesel engine combustion and emissions. Energ. Convers. Manag. **49**, 1696–1704 (2008)

32. Alzueta, M.U., Finestra, M., Bilbao, R.: Methanol oxidation and its interaction with nitrogen oxide. Energy Fuels **15**, 724–729 (2001)

33. Alzueta, M.U., Hernández, J.M.: Ethanol oxidation and its interaction with nitric oxide. Energy Fuels **16**, 166–171 (2002)

34. Glarborg, P., Alzueta, M.U., Kjaergaard, K., Dam-Johansen, K.: Oxidation of formaldehyde and its interaction with nitric oxide in a flow reactor. Combust. Flame **132**, 629–638 (2003)

35. Alzueta, M.U., Borruey, M., Callejas, M.A., Millera, A., Bilbao, R.: An experimental and modeling study of the oxidation of acetylene in a flow reactor. Combust. Flame **152**, 377–386 (2008)

36. Alzueta, M.U., Aranda, V., Monge, F., Millera, A., Bilbao, R.: Oxidation of methyl formate and its interaction with nitric oxide. Combust. Flame **160**, 853–860 (2013)

37. Kee, R.J., Rupley, F.M., Miller, J.A.: Chemkin-II: A fortran chemical kinetics package for the analysis of gas-phase chemical kinetics, Sandia National Laboratories. SAND89-8009B (1989)

38. CHEMKIN-PRO 15131, Reaction Design, San Diego (2013)

39. Bilbao, R., Alzueta, M.U., Millera, A.: Experimental study of the influence of the operating variables on natural gas reburning efficiency. Ind. Eng. Chem. Res. **34**, 4531–4539 (1995)